

Dynamics and Mechanism of DNA Repair in a Biomimetic System: Flavin–Thymine Dimer Adduct

Ya-Ting Kao, Qin-Hua Song, Chaitanya Saxena, Lijuan Wang, and Dongping Zhong*

Department of Physics, Department of Chemistry and Biochemistry, and Programs of Biophysics, Chemical Physics, and Biochemistry, The Ohio State University, Columbus, Ohio 43210, United States

S Supporting Information

ABSTRACT: To mimic photolyase for efficient repair of UV-damaged DNA, numerous biomimetic systems have been synthesized, but all show low repair efficiency. The molecular mechanism of this low-efficiency process is still poorly understood. Here we report our direct mapping of the repair processes of a flavin–thymine dimer adduct with femtosecond resolution. We followed the entire dynamic evolution and observed direct electron transfer (ET) from the excited flavin to the thymine dimer in 79 ps. We further observed two competitive pathways, productive dimer ring splitting within 435 ps and futile back-ET in 95 ps. Our observations reveal that the underlying mechanism for the low repair quantum yield of flavin–thymine dimer adducts is the short-lived excited flavin moiety and the fast dynamics of futile back-ET without repair.

One of the detrimental effects of UV radiation on the biosphere is the formation of cyclobutane pyrimidine dimers (CPDs), which causes DNA damage and can lead to skin cancer. Photolyase is a photoenzyme that is responsible for repairing UV-damaged DNA in many organisms.¹ In our recent studies on *Escherichia coli* CPD photolyase,^{2,3} we captured the radical intermediates and revealed the electron-transfer (ET) mechanism in DNA repair. Upon excitation with blue light, CPD photolyase, a flavin-containing enzyme, transfers an electron from the isoalloxazine ring of cofactor FADH⁻ to the dimer. The cyclobutane ring then splits spontaneously, with subsequent electron return to restore the active form of cofactor FADH⁻. The DNA repair by photolyase is very efficient, with a quantum yield of 0.80–0.95.^{1,3} Numerous biomimetic systems have been synthesized to mimic the repair function, but all have shown low repair efficiency, for example, 0.016–0.062 for flavin–thymine dimer systems^{4,5} and 0.06–0.40 for indole–thymine dimer systems.^{6,7} The molecular mechanisms of these low-efficiency processes have not been understood.^{8,9} Here we report our direct mapping of the repair processes in a biomimetic flavin–thymine dimer adduct by following the temporal evolution of reactants and intermediates using femtosecond spectroscopy. By capturing the complete repair photocycle and comparing it to that of CPD photolyase, we can understand how CPD photolyase achieves its high repair efficiency.

Instead of simply using a solution mixture of thymine dimer and flavin, we employed a covalent linkage between the lumiflavin (LF) and thymine dimer (T<>T) to hold the flavin

photosensitizer and dimer together (Figure 1). The oxidized flavin–thymine dimer adduct (LF–T<>T) was synthesized,

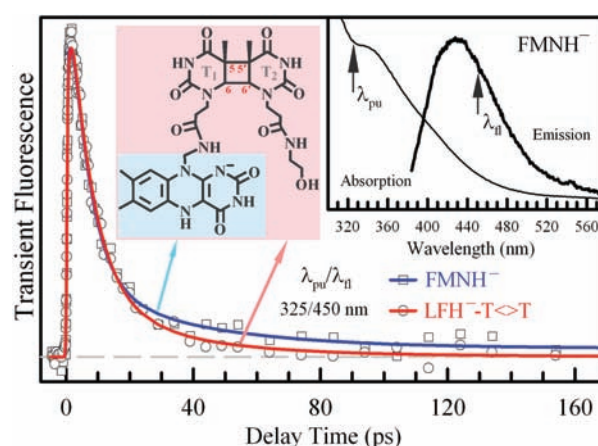


Figure 1. Femtosecond-resolved fluorescence transients of reduced FMNH⁻ and LFH–T<>T gated at 450 nm upon 325 nm excitation. The molecular structures of LFH–T<>T and LFH⁻ are highlighted in pink and blue, respectively, in the left inset. The right inset shows the absorption and emission spectra (360 nm excitation) of reduced FMNH⁻. The two arrows indicate the pump wavelength (λ_{pu}) and gated fluorescence emission wavelength (λ_{fl}).

purified, and characterized as described previously.⁵ The fully reduced flavin–thymine dimer (LFH–T<>T) and the fully reduced flavin (FMNH⁻) were generated from 350 μ M oxidized samples through chemical reduction¹⁰ with 250 mM sodium borohydride in 12.5 mM phosphate buffer (pH 8.5) under anaerobic conditions. Complete reduction was confirmed by both the UV–vis absorption and, more importantly, the fluorescence spectrum, which contained a single emission peak, indicating a single species without a mixture of different redox flavins. The molecular structures of LFH–T<>T and LFH⁻ are highlighted in pink and blue, respectively, in the left inset of Figure 1. The absorption and emission spectra of fully reduced FMNH⁻ in solution are shown in the right inset of Figure 1. The absorption spectrum is consistent with the results of previous studies,^{4,11} and the emission spectrum is similar to that in our earlier report on FADH^{*} emission.¹² Upon 360 nm excitation, we observed weak fluorescence emission peaked at 435 nm for fully reduced FMNH⁻. More importantly, we

Received: December 1, 2011

Published: January 4, 2012

observed the excitation-wavelength dependence of the emission spectra.¹² Also, the fluorescence intensity of fully reduced flavin in solution is much weaker than that observed in photolyase,¹² suggesting very different dynamic behaviors of fully reduced flavin in the two environments (see below).

We first characterized the excited FMNH^{*} dynamics using femtosecond-resolved fluorescence spectroscopy. When the weak FMNH^{*} emission at 450 nm was monitored, the fluorescence transient in the absence of dimer exhibited multiple decay dynamics with lifetimes (τ_d) of 5.8 ps (82%), 35 ps (16%), and 1.5 ns (2%), as shown in Figure 1. Such multiple-decay dynamics reflects the ultrafast deactivation of the excited FMNH^{*}.¹² In contrast to excited FMNH^{*} in solution, our previous studies² showed the dynamics of the excited FADH^{*} in photolyase to have a dominant long lifetime of 1.3 ns and suggested that the butterfly bending of the isoalloxazine ring is a critical motion that directly controls the excited-state dynamics of fully reduced flavins.¹² In solution, free LFH^{*} easily changes its conformation, whereas in the proteins it is highly restricted, geometrically and electrostatically. Thus, the more flexible the environment, the shorter the excited-state lifetime of fully reduced flavin.

In the presence of the thymine dimer, the fluorescence transient exhibits faster dynamics, indicating the presence of another reaction channel, the ET reaction. The reduction potential for flavin (FMNH^{*}/FMNH⁻) is -0.172 V vs NHE,¹³ and that for thymine dimer ($T<>T/T<>T^-$) is -1.96 V vs NHE.¹⁴ Using the 500 nm absorption tail as the 0–0 transition energy of 2.48 eV, we obtained a net ΔG° of -0.692 eV. Thus, the intramolecular ET between the excited flavin and the thymine dimer is energetically favorable. By considering the ET reaction in each deactivation process of excited LFH^{*} (Figure 1), we obtained an ET dynamics lifetime (τ_{ET}) of 79 ps. Thus, the quantum yields of ET, calculated as $\tau_{ET}^{-1}/(\tau_{ET}^{-1} + \tau_d^{-1})$, were found to be 0.068, 0.307, and 0.950, respectively, for the three deactivation processes, giving a first-step ET quantum yield (ϕ_{ET}) of 0.124. In photolyase, even though the average ET dynamics is slower ($\tau_{ET} = 250$ ps vs 79 ps), the long-lived (1.3 ns) excited flavin (FADH^{*}) results in a much higher ET quantum yield of ~ 0.85 .^{2,3,15,16} This observation reveals that the ultrafast deactivation of the excited fully reduced flavin in all biomimetic flavin–thymine dimer adducts already leads to a low quantum yield in the first-step forward ET.

According to recent quantum-chemical calculations,^{8,9,17,18} the splitting of the C5–C5' bond of the anionic thymine dimer ($T<>T^-$) is a downhill reaction that occurs in less than 1 ps (τ_{SP1}), as indicated in Figure 2A. The C5–C5' bond splitting in photolyase was determined to occur in less than 10 ps.^{3,16} This step was too fast to be observed here because the intermediate could not be accumulated as a result of the long formation time (79 ps). After the C5–C5' ultrafast splitting, the reaction can evolve along one of two pathways: (1) the nonproductive pathway including back ET (τ_{BET}) and ring reclosure without repair or (2) the repair channel including C6–C6' bond splitting (τ_{SP2}) and then electron return after repair (τ_{ER}). On the basis of our recent studies on thymine dimer repair by photolyase using UV–vis detection, the C6–C6' splitting is decoupled from the electron return.³ For clarity, we here describe the LFH^{*} formed after the C5–C5' bond splitting as the initially formed LFH^{*} (underlined in cyan in Figure 2A) and the LFH^{*} formed after the C6–C6' splitting as the branched LFH^{*} (underlined in purple in Figure 2A).

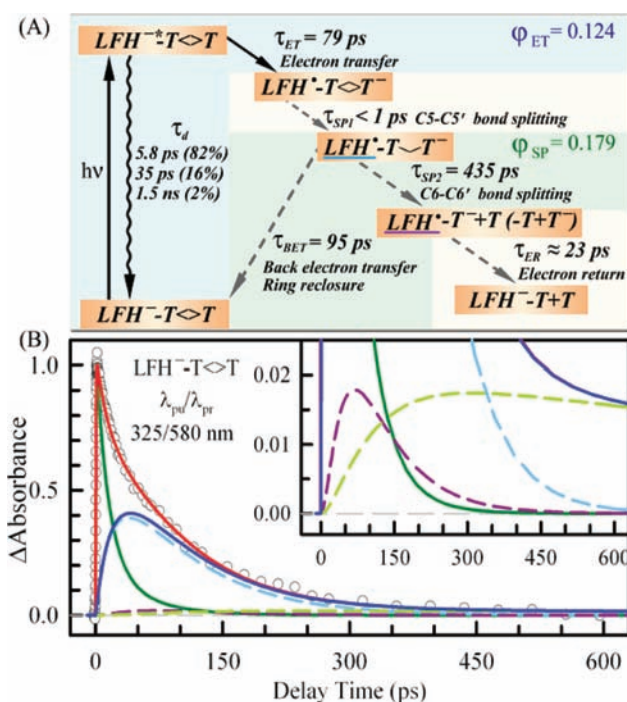


Figure 2. (A) Repair scheme with forward ET (τ_{ET}) after light excitation, ultrafast first C5–C5' bond splitting (τ_{SP1}) and ring reclosure without repair, and the repair channel including C6–C6' bond splitting (τ_{SP2}) and electron return (τ_{ER}). (B) Femtosecond-resolved absorption signal of LFH^{*}–T<>T probed at 580 nm upon 325 nm excitation, with detection of both LFH^{*}–T<>T (green curve; mainly probed at 710 nm) and LFH^{*} (blue curve). The total LFH^{*} signal is from the one dominant contribution of the initially formed LFH^{*} (dashed cyan curve) and two minor contributions of the branched LFH^{*} in the repair channel ($\geq 85\%$, dashed purple; $< 15\%$, dashed lime-green). A minor plateau from the deactivation channels in the 710 nm transient was removed for clarity. The inset shows the dynamics of the two fitted minor channels.

With knowledge of the forward ET dynamics of LFH^{*}–T<>T, we were able to map out the temporal evolution of LFH^{*} by probing at wavelengths from 580 to 710 nm to follow the CPD repair. For example, we observed similar transients upon probing at 580 and 625 nm, due to the capture of the radical LFH^{*} (blue curve in Figure 2B); these were drastically different from that probed at 710 nm (Figure 2B). With probing at 580 nm, we observed three different dynamic components of LFH^{*} (the kinetic fitting model is given in the Supporting Information). The dominant one is from the initially formed LFH^{*}, with a decay dynamics lifetime of 78 ps [$(\tau_{SP2}^{-1} + \tau_{BET}^{-1})^{-1}$ in Figure 2A and dashed cyan curve in Figure 2B]. In our recent studies of an indole–thymine dimer adduct through transient absorption in the UV range, we observed dimer splitting in 450 ps (τ_{SP2}) in aqueous solution. Here, with probing at 580 nm, we obtained dimer splitting in 435 ps (τ_{SP2}) and back ET in 95 ps (τ_{BET}). Two minor LFH^{*} components from the branched LFH^{*} were also observed (dashed purple and lime-green curves in Figure 2B). For the minor component with more than 85% of the total branched LFH^{*} signal, we observed formation mainly in $\tau_{ER} = 23 \pm 12$ ps and a complex decay (dashed purple curve in the Figure 2B inset) mainly in ~ 78 ps. The 23 ps lifetime is actually for the electron return (ER) process. The slower formation and faster decay result in apparent reverse kinetics and less LFH^{*} accumulation. The τ_{ER} of 23 ps is for the ER from linked

thymine T_1 (Figure 1 inset) to LFH^{\bullet} to restore the active form LFH . The other minor component contributing less than 15% exhibits a long plateau (dashed lime-green curve in the Figure 2B inset), indicating that the negative charge could stay in the distant thymine T_2 , leading to a long-lived LFH^{\bullet} . With probing at 710 nm, we observed the dominant LFH^{\bullet} signal and a minor LFH^{\bullet} signal with similar dynamics probed at 580 and 620 nm.

Knowing that the reduction potential for thymine base (T/T^-) is -1.90 V vs NHE,¹⁴ we obtained a net ΔG° of -1.728 eV for ER. On the basis of the net ΔG° values and the rates of both ET and ER, we estimate that the distance between the flavin and the thymine dimer is ~ 7 Å and that the reorganization energy is ~ 1.5 eV.¹⁶ Hence, the ET reaction lies in the Marcus normal region and the ER reaction in the inverted region. Also, the faster dynamics of ER in comparison with ET is due to a low activation energy and might also be facilitated through hot vibrational modes of the products.^{19–22} For back ET, because it occurs along the splitting coordinate and its free energy is greatly reduced during the splitting, the absolute value of the net ΔG° should be much smaller than 1.788 eV (-1.96 eV + 0.172 eV = -1.788 eV).^{8,9} Thus, back ET probably lies in the normal region with a small driving force,^{8,16} resulting in the lifetime of 95 ps, which indicates that back ET is slower than ET and ER.

The fast back ET of 95 ps in solution indicates a relatively unstable charge-separated intermediate ($LFH^{\bullet}-T^{<>T^-$), leading to a significant competition between ring splitting (435 ps) and futile back ET. The efficiency of the dimer ring splitting with ER is 0.179 [$\phi_{SP} = \tau_{BET}/(\tau_{SP2} + \tau_{BET})$]. Considering the ET quantum yield of 0.124 (ϕ_{ET}) acquired from the fluorescence experiment, we obtained the total repair efficiency of 0.022 ($\Phi_{total} = \phi_{ET}\phi_{SP}$) which is about one-third of the reported value obtained from steady-state measurements (0.062), but on the same order.⁴ Our observations reveal that the underlying molecular mechanism for the low repair quantum yield of all flavin–thymine dimer adducts is the short-lived excited flavin and the fast dynamics of futile back ET. In contrast, in CPD photolyase, the enzyme can utilize geometric restriction and electrostatic interactions to confine the flavin cofactor and lengthen its excited-state lifetime. This long-lived cofactor could exist long enough to react with CPDs to form a charge-separated intermediate and thus reach a high ET quantum yield. Moreover, the active site stabilizes the charge-separated intermediate in photolyase (>1 ns) and speeds up the ring splitting, which occurs within 90 ps.³ Such modulation of the dynamics leaves enough time to cleave the ring, resulting in a high splitting efficiency. These two high-efficiency processes lead to perfect repair of damaged DNA by photolyase.

■ ASSOCIATED CONTENT

📄 Supporting Information

Summary of the kinetic fitting model. This material is available free of charge via the Internet at <http://pubs.acs.org>.

■ AUTHOR INFORMATION

Corresponding Author

zhong.28@asc.ohio-state.edu

■ ACKNOWLEDGMENTS

This work was supported in part by NIH Grant GM074813 and a Packard Foundation Fellowship to D.Z.. The authors thank Dr. Xunmin Guo for helpful discussions.

■ REFERENCES

- (1) Sancar, A. *Chem. Rev.* **2003**, *103*, 2203–2237.
- (2) Kao, Y.-T.; Saxena, C.; Wang, L.; Sancar, A.; Zhong, D. *Proc. Natl. Acad. Sci. U.S.A.* **2005**, *102*, 16128–16132.
- (3) Liu, Z.; Tan, C.; Guo, X.; Kao, Y.-T.; Li, J.; Wang, L.; Sancar, A.; Zhong, D. *Proc. Natl. Acad. Sci. U.S.A.* **2011**, *108*, 14831–14836.
- (4) Epple, R.; Wallenborn, E.-U.; Carell, T. *J. Am. Chem. Soc.* **1997**, *119*, 7440–7451.
- (5) Song, Q.-H.; Tang, W.-J.; Ji, X.-B.; Wang, H.-B.; Guo, Q.-X. *Chem.—Eur. J.* **2007**, *13*, 7762–7770.
- (6) Song, Q.-H.; Tang, W.-J.; Hei, X.-M.; Wang, H.-B.; Guo, Q.-X.; Yu, S.-Q. *Eur. J. Org. Chem.* **2005**, 1097–1106.
- (7) Kim, S.-T.; Hartman, R. F.; Rose, S. D. *Photochem. Photobiol.* **1990**, *52*, 789–794.
- (8) Hassanali, A. A.; Zhong, D.; Singer, S. J. *J. Phys. Chem. B* **2011**, *115*, 3848–3859.
- (9) Hassanali, A. A.; Zhong, D.; Singer, S. J. *J. Phys. Chem. B* **2011**, *115*, 3860–3871.
- (10) Müller, F.; Massey, V.; Heizmann, C.; Hemmerich, P.; Lhoste, J.-M.; Gould, D. C. *Eur. J. Biochem.* **1969**, *9*, 392–401.
- (11) Ghisla, S.; Massey, V.; Lhoste, J.-M.; Mayhew, S. G. *Biochemistry* **1974**, *13*, 589–597.
- (12) Kao, Y.-T.; Saxena, C.; He, T.-F.; Guo, L.; Wang, L.; Sancar, A.; Zhong, D. *J. Am. Chem. Soc.* **2008**, *130*, 13132–13139.
- (13) Draper, R. D.; Ingraham, L. L. *Arch. Biochem. Biophys.* **1968**, *125*, 802–808.
- (14) Scannell, M. P.; Fenick, D. J.; Yeh, S.-R.; Falvey, D. E. *J. Am. Chem. Soc.* **1997**, *119*, 1971–1977.
- (15) Kao, Y.-T.; Saxena, C.; Wang, L.; Sancar, A.; Zhong, D. *Cell Biochem. Biophys.* **2007**, *48*, 32–44.
- (16) Liu, Z.; Guo, X.; Tan, C.; Li, J.; Kao, Y.-T.; Wang, L.; Sancar, A.; Zhong, D. *J. Am. Chem. Soc.* **2012**, submitted for publication.
- (17) Masson, F.; Laino, T.; Tavernelli, I.; Rothlisberger, U.; Hutter, J. *J. Am. Chem. Soc.* **2008**, *130*, 3443–3450.
- (18) Saettel, N. J.; Wiest, O. *J. Am. Chem. Soc.* **2001**, *123*, 2693–2694.
- (19) Jortner, J.; Bixon, M. *J. Chem. Phys.* **1988**, *88*, 167–170.
- (20) Nagasawa, Y.; Yartsev, A. P.; Tominaga, K.; Bisht, P. B.; Johnson, A. E.; Yoshihara, K. *J. Phys. Chem.* **1995**, *99*, 653–662.
- (21) Barbara, P. F.; Meyer, T. J.; Ratner, M. A. *J. Phys. Chem.* **1996**, *100*, 13148–13168.
- (22) Gladkikh, V.; Burshtein, A. I.; Feskov, S. V.; Ivanov, A. I.; Vauthey, E. *J. Chem. Phys.* **2005**, *123*, No. 244510.